

1 A theoretical model for shallow failure on unconsolidated soil slope 2 considering overland and interstitial flow

3 Chao-xu Guo ^{a, b}, Jia-wen Zhou ^{c, d}, Peng Cui ^{a*}, Yu Lei ^{a, b}, Ming-hui Hao ^d, Fu-gang Xu ^d

4 ^a Key Laboratory of Mountain Hazards and Surface Process, Institute of Mountain Hazards and Environment, Chinese Academy of Sciences,
5 Chengdu, Sichuan 610044, China

6 ^b University of Chinese Academy of Science, Beijing, 100049, China

7 ^c State Key Laboratory of Hydraulics and Mountain River Engineering, Sichuan University, Chengdu, Sichuan 610065, China

8 ^d College of Water Resources & Hydropower, Sichuan University, Chengdu, Sichuan 610065, China

9 (*Corresponding author: pengcui@imde.ac.cn)

10 Abstract

11 Shallow failure, always appearing on unconsolidated slope especially after earthquake, is the main source of
12 debris flow. It is imperative to approach the initiation mechanism and model of the shallow failure from
13 unconsolidated soil. Through flume experiments for unconsolidated soil with rainfall and thin surface water flow,
14 the results show that interstitial flow would bring away fine particles which may stop, accumulate, block pore in
15 soil and cause soil strength reducing with pore water pressure increasing due to formation of local impermeable
16 layer; Overland flow can cause shear stress on the slope surface. The coupling effect is often resulting in
17 shallow failure with widely graded and unconsolidated soil. And the interstitial flow which is always neglected
18 plays more important role than the overland flow. Based on the failure mechanism analysis, a new theoretical
19 model for the shallow failure was established by incorporating hydrodynamic theory considering the superficial
20 shear and fine particle migration effect. This model was validated by examples and proved to be suited better for
21 unconsolidated soil failure analysis. In addition, the mechanism analysis and the established model can provide
22 a new direction and deeper understanding of shallow failure with unconsolidated soil.

23 **Keywords:** Unconsolidated soil; Surface water flow; Shallow failure; Hydrodynamics; Fine particle migration;

24 **1. Introduction**

25 Rainfall-induced failures pose significant hazards in many parts of the world especially in mountainous areas
26 with rainy environments. Among hazardous rainfall-induced failures, shallow failures are often occurring to
27 cause direct disaster or transforming into dangerous debris flow accompanying with unexpected appearance
28 characterized by rapid movement and large runout distance (Gabet, 2006;). So the mechanism and precise
29 numerical model are meaningful to apprehend this process for disaster prevention and mitigation.

30 There have been some experimental and analytical studies on the mechanism of rainfall-induced slope
31 failures. On one hand, groundwater table rise under rainfall would increase pore water pressure, reduce the soil
32 strength, and lead to Coulomb failure or liquefaction. Iverson (1997, 2000) regarded that densely packed soils
33 dilate to reach the critical failure state, and loosely packed soils works on the contrary. Contraction can elevate
34 pore pressures if the rate of pore-space reduction surpasses the rate at which induced water pressures can
35 dissipate. Pore pressures elevated in this manner can produce classical liquefaction, and this type of liquefaction
36 or near-liquefaction has been suggested as a mechanism for debris-flow mobilization. With small-scale
37 experiment, Huang et al (2008, 2009) has found retrogressive shallow slope failures were initiated by the
38 collapse and wash-out of the slope toe, which resulted from the saturation of the soil-bedrock interface, the
39 lateral interflow along the soil-bedrock interface, and the build-up of pore water pressures or the mounding of a
40 groundwater table around the slope toe. On the other hand, thin water flow or small amounts of runoff induced
41 by rainfall would also lead to a water-saturated inertial grain flows governed by Bagnold's (1954) concept of
42 dispersive stress when the shear stress is more than yield stress. Takahashi's failure is essentially a Coulomb
43 failure with consideration of the hydrodynamic shear effect. However, thees two types of mechanisms are
44 ambiguous in failure and neglect the fine particles migration effect which is a characteristic of widely graded or
45 unconsolidated soil.

46 Shallow failure is most often addressed by an infinite slope stability analysis which Coulomb failure of
47 infinite slopes with homogeneous, isotropic soil. In the case of widely graded soil, the cohesion is 0 . And it is a
48 convenient mathematical idealization used to specify an inclined, tabular soil mass with lateral dimensions much
49 greater than its thickness. Lade (2010) proposed a power function failure criterion to express effective cohesion
50 which can be used in a closed form expression for the factor of safety for shallow failure. Takahashi considers
51 the failure mechanism of loose soil to be formed under a condition in which the shear stress is larger than the
52 resisting stress, and he proposed a formula that is based on the failure depth under surface runoff and without
53 surface runoff (Takahashi, 2007). Based on laboratory experiments and field observations, Wang and Zhang

54 (1990) considered strong erosion to be the main cause of soil failure. Using fluid mechanics theory, they
55 obtained a flow movement equation for the deposit surface and shear stress, which is regarded as extending
56 Takahashi's model in-depth. However, these authors ignored the influence of the pore water pressure on the
57 shearing strength and those parameters that could change with time. Iverson et al (1997) established infinite
58 slope failure model which can consider alternative pore-pressure distributions (groundwater head gradient in an
59 arbitrary direction) and the potential for soil liquefaction. Zhou (2013) considers the surface runoff and seepage
60 process in the slope stability analysis of slope failure meanwhile neglects dynamic effects such as hydraulic
61 shear force and fine particle migration. Moreover, some statistical models are presented based on many
62 laboratory and field experiments (Cui, 1992; Gregoretti and Fontana, 2008; Tognacca et al., 2000). However, the
63 results from these models could have little application which neglect the grain size distribution and have
64 difficulties in searching sliding face.

65 Based on laboratory experiments and field investigations, flume experiments with rainfall and thin water flow
66 conditions are carried out to study shallow failure mechanism with widely graded and unconsolidated soil.
67 Hydrodynamic effects such as hydraulic shear and fine particle migration have been proposed for theoretical
68 model constructing. Model presented in this paper is validated by experiment data and compared with classic
69 model in the end.

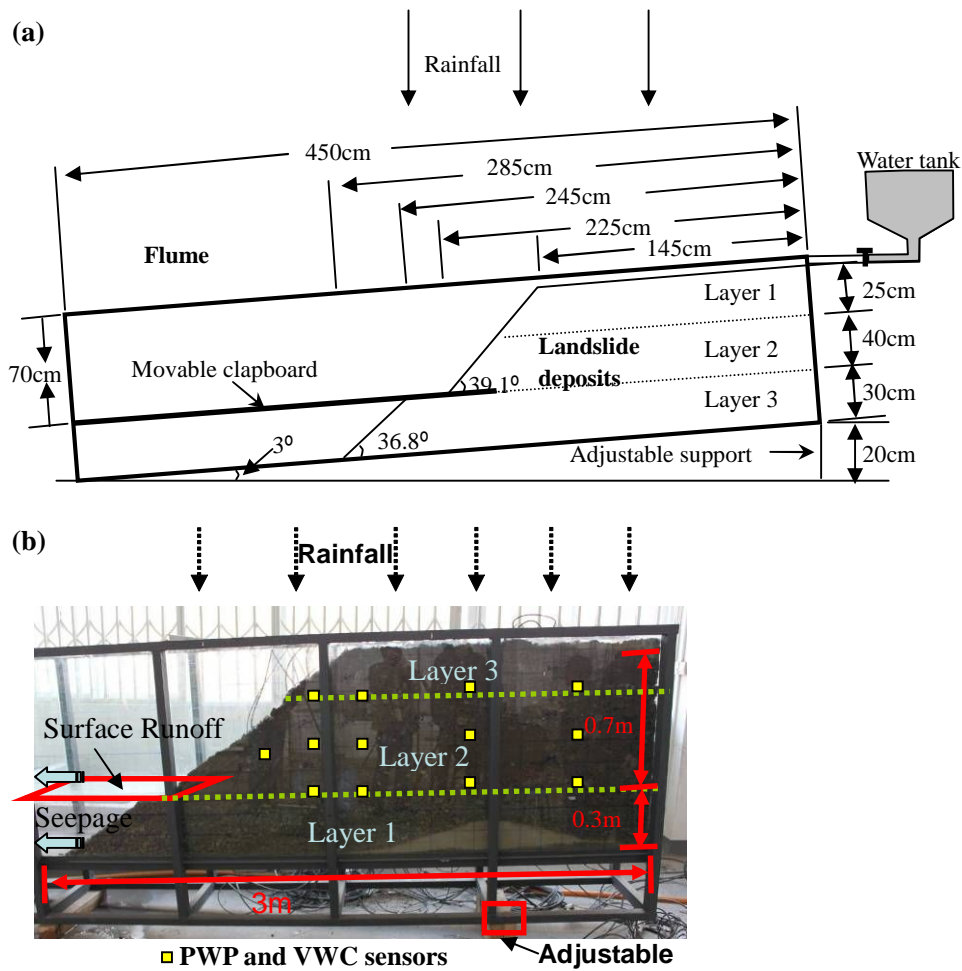
70 **2. Flume experiment for unconsolidated soil**

71 Generally, interstitial flow is commonly happening within the slope under rainfall. In the mountain area,
72 overland flow is also generated from excessive rain water. Here, we design an artificial rainfall and **water tank** to
73 simulate the interstitial flow and overland flow. Two conditions which are rainfall only and overland flow plus
74 rainfall are adopted to study the failure mechanism with widely graded **and unconsolidated soil**.

75 *2.1. Experimental design*

76 We took the unconsolidated soil from the Wenjiagou Gully in Qingping area, southwestern China as the
77 sampled soil, with conditions of rainfall intensity of 140 mm/h (the rainfall intensity that occurs every 5 years in
78 this area is 70 mm/h), slope angle 39.1°, bed gradient 3° and 6°, and rainfall duration of 3 hours. An artificial
79 rainfall system and flume and monitoring sensors are shown in Figure 1. **And it is designed for separating**
80 **surface runoff and seepage. Meanwhile, water flow of approximately 1.70 m/s and 0.05 m in depth sustained by**
81 **a water tank is used to simulate thin sheet flow on the slope.** A total of 12 sets of pore water pressure and

82 volumetric water content sensors were installed in the slope.



83

84

85 **Figure 1.** Schematic design and actual shape of the flume: (a) schematic design of the flume (side view) and (b)
 86 artificial rainfall test equipment for unconsolidated soil (PWP and VWC are the pore water pressure and
 87 volumetric water content, respectively)

88 Table 1 shows the particle size distribution of the soil samples that are used in the artificial rainfall tests
 89 (particles larger than 60 mm are excluded from the test).

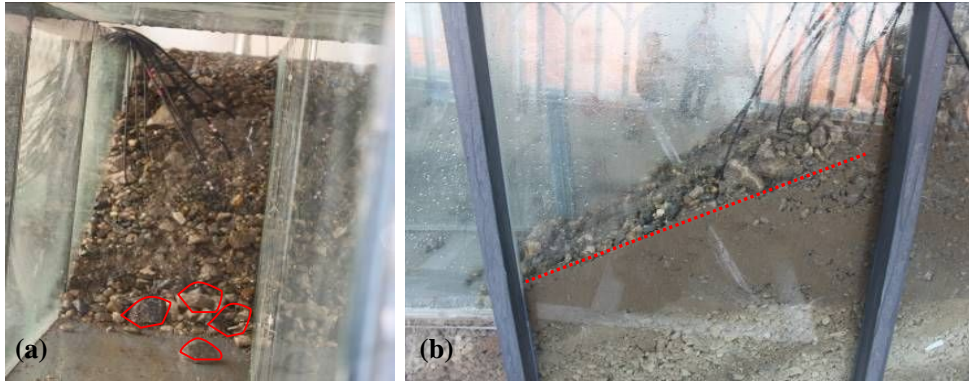
90

Table 1. Particle size distribution characteristics of the soil used in the experimental test

| Grain size(mm) | Cumulative ratio (%) | | |
|----------------|----------------------|--------------|-------------|
| | First layer | Second layer | Third layer |
| <60 | 100 | 100 | 100 |
| <40 | 100 | 90 | 82 |
| <20 | 40 | 60 | 72 |
| <5 | 10 | 28 | 40 |
| <2 | 10 | 18 | 10 |

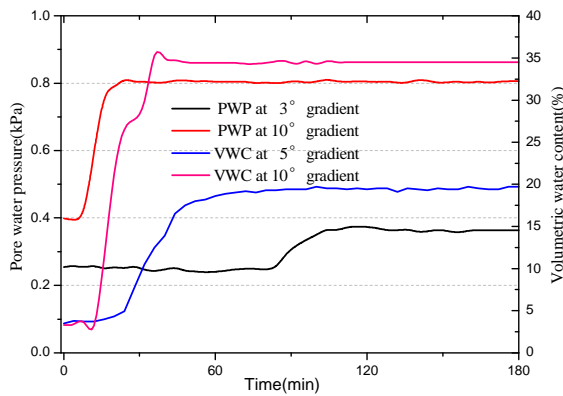
91 2.2. Flume experiment with rainfall only

92 When the unconsolidated slope is under the rainfall condition, only small shallow slope failures occur, such as
93 particle tumbling, localized slides or collapse in the whole rainfall process (see Figure 2). Here, the rainfall
94 intensity is 140mm/h, which is sufficiently large, but no significant slope failure or debris flow occurs.



95
96 **Figure 2.** Shallow failure of the unconsolidated slope under a strong rainfall condition: (a) particle movements
97 and small slide (front view) and (b) grain coarsening (side view)

98 To find out the reason why no large slope failure and debris flow occurred, variations of the pore water
99 pressure (PWP) and volumetric water content (VWC) at the slope toe are measured, as illustrated in Figure 3.



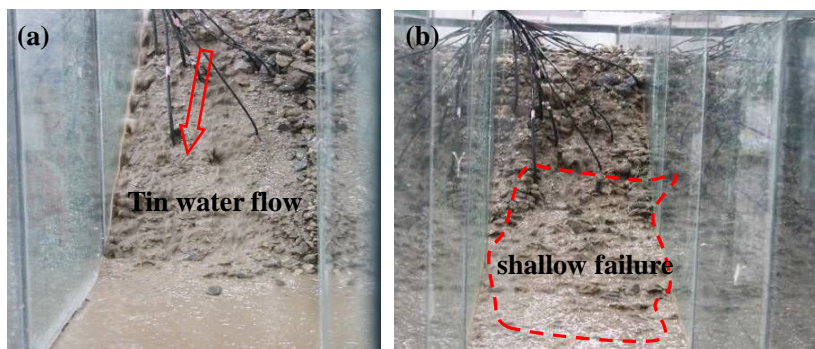
100
101 **Figure 3.** Variations in the pore water pressure and volumetric water content at slope toe during the rainfall
102 process

103 As shown in Figure 3, PWP and VWC variations can be summarized into three stages during the 2 hour
104 rainfall: (1) the initial steady stage, (2) sharp increasing stage and (3) final steady stage. At a higher gradient of
105 6°, the soil could reach stage 2 and 3 about 50 mins earlier than it is at a lower gradient of 3°. With the gradient
106 increasing, the water-holding capacity of the loose deposit decreases, and water flows out more rapidly, which
107 leads to the water content increasing (reaching 34.5% with a 6° gradient at T=180 min), and the surface soil of
108 the slope is almost saturated. However, the pore water pressure at the slope toe is approximately 0.8 kPa, and

109 might not be large enough to induce slope toe failure or regressive failure. There are no large-scale soil failures
110 except minor shallow failures. The results demonstrated that shallow failures are strongly linked to surface
111 runoff, interflow and fine particle migration, which greatly improves our understanding of the mechanisms
112 behind shallow slope failures (Cui et al, 2014).

113 2.3. Flume experiment with thin water flow plus rainfall

114 Thin water flow is very common on slope in the field. However, in the experiment, due to the size effect of
115 flume, the thin overland flow is difficult to model by artificial raining system. Therefore, water flow at 1.7 m/s
116 and a depth of 5 cm applied by a water tank in addition to the artificial rainfall condition above.



117
118 **Figure 4.** Shallow failure with superficial thin water flow: (a) surface water flow along the slope surface (front
119 view) and (b) slope state after shallow failure

120 It is found that the deeper sensors (PWP and VWC) show fluctuations while the soil failure happens, which
121 corresponds with the previous findings (Iverson, 2000; Chen, 2006). Experimental tests shown in Figure 4
122 indicate that the soil failure is occurring at the shallow layer, about 5cm. This failure is so minor that it is usually
123 regarded as a type of erosion (Bryan, 2000). In fact, erosion is the slow movement of a small amount of particles,
124 and may last for a few minutes to even a few years, such as sheet wash, rill erosion, piping erosion, etc.
125 However, in our case, we consider it as a small scale slope failure at a shallow position. When thin water flows
126 across the slope, fine particles are first to detach and liquefy (the maximum flow concentration reaches about
127 $1.8\text{g}/\text{cm}^3$). At the same time, surficial flow entrains surface particles, leading to shallow landslide. Then debris
128 flow is easily triggered along the slope surface, with abundant loose particle material and water flow. This
129 process also indicates that initiation of the debris flow is not a simple erosion failure but a complex chain action
130 with various transformations.

131 In summary, with thin water flow and rainfall, the unconsolidated soil are more prone to failures, such as the
132 shallow landslide, flowslide, and even development of debris flow than with rainfall alone. At the process of

133 shallow failure, fine particles migrate with hydrodynamic force vertically apart from along the slope surface,
134 which is verified by grading analysis of the slope after the experiment. From the grading curve, we find that the
135 fine particles (<2mm) increase from 18% to 23%, which shows their great influence on the slope failure
136 especially the shallow failure. A similar conclusion can also be found in flume tests with rainfall (Cui et al.,
137 2014).

138 3. Initiation mechanism and numerical model for the debris flow

139 3.1. Shallow failure mechanism

140 Comparing the slope physics properties before and after the test under rainfall condition, the cohesion
141 decreases sharply, as shown in Table 2. In fact, the materials in our experiment contain some clay (Based on the
142 laser-phase Doppler analyzer, the clay percent content is about 5%), therefore show a little cohesion. In the
143 experiment, the superficial fine particle is migrating from surface towards the inside of the slope, associated
144 with the change of grading in superficial soil. As the clay decreasing, the superficial soil will show a nearly-zero
145 cohesion but lightly reduction in internal friction angle.

146 In fact, with interstitial flow by rainfall, there are two effects: on one hand, fine particles (less than 2mm)
147 migration leads to a coarse layer (the surface soil is in a saturated state and its cohesion is close to zero); on the
148 other hand, the moving fine particles block the soil pores and cause saturation of the top soil, increased pore
149 water pressure and uplift pressure, and decreased soil shear strength. Moreover, the fine particles liquefying and
150 integrating into water flow will increase the viscosity and enhance the hydrodynamic effect. However, this effect
151 is usually ignored in our research.

152 Besides the hydrodynamic effect, soil shear strength will be reduced by the coarse particle gradation. And a
153 perched water table and water film will form with the pores blocked, and then provide lubrication (Lu and Cui,
154 2010a, b). Though the superficial soil strength decreased sharply with interstitial flow by rainfall, only small and
155 shallow failure occurred on the slope.

156 **Table 2.** Shear strength parameters of unconsolidated soil at different water content conditions

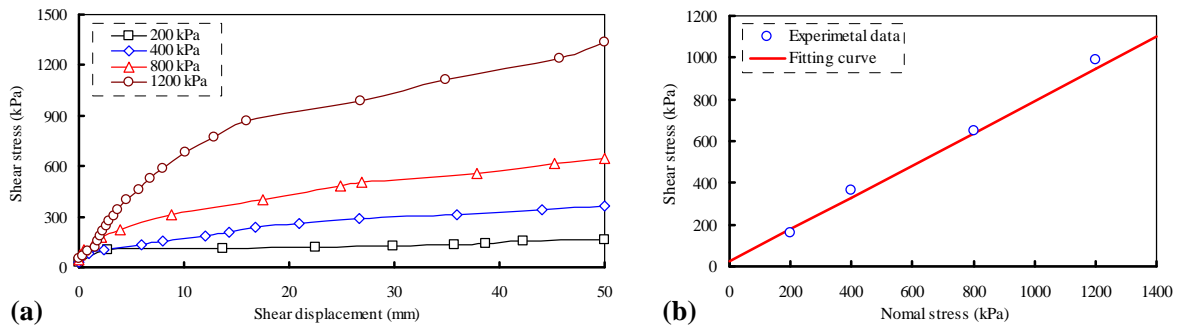
| Shear strength parameter | Unsaturated soil (water content 4.5%-6.5%) | Saturated soil (water content 15%-17%) | Natural soil (water content 1.0%-2.0%) |
|--------------------------|---|---|---|
| Cohesion (kPa) | 22.3 | ~0 | 42.5 |
| Friction angle (°) | 37.6 | 32.3 | 38.1 |

157

158 With thin overland flow plus rainfall condition, besides the failure mechanism above, water flow shear stress

159 is increasing and triggering larger scale failure. Soil will disintegrate in a moment, or enter into the water flow
160 (the liquidation and suspension effect), move down along the slope, with the loose material come together, and
161 develop into debris flow. In the field, with steep terrain, suitable hydrodynamic conditions, and a large motion
162 distance, the huge debris flow triggered in the channel will cause major disasters such as the Wenjiagou debris
163 flow in 2010 (Zhou, 2013).

164 To verify the important role of hydrodynamic effect by thin overland flow, after the experiment with rainfall,
165 the shear strength parameters of unconsolidated soil are tested by direct shear testing under four normal stress
166 conditions (200kPa, 400kPa, 800kPa and 1200kPa), as shown in Figure 5. The sample is the soil taken from the
167 flume after the test, which has a density of 1.909 g/cm^3 and water content of 4.5%-6.5% (approximately). The
168 water content of natural soil is about 1.0%-2.0% and for saturated soil is about 15%-17%.



169 (a) (b)
170 **Figure 5.** Test results of the shear strength for unconsolidated soil: (a) variation in the shear stress with the shear
171 displacement and (b) shear strength parameters of the unconsolidated soil

172 Experimental results show that the cohesion and friction angle for unsaturated soil (water content 4.5%-6.5%)
173 are 22.3 kPa and 37.6° , respectively, and 42.5 kPa and 38.1° for natural soil (water content 1.0%-2.0%).
174 Laboratory tests indicate that the cohesion reduced sharply with both thin water flow and rainfall, but the
175 friction angles barely changed. For the saturated soil behind the surface water flow, the cohesion is assumed
176 equal to 0, and the friction angle is determined by the experimental test for unconsolidated soil when the water
177 content is 15%-17%. Table 2 summarizes the shear strength parameter of unconsolidated soil in different water
178 content conditions, which are used for numerical analysis.

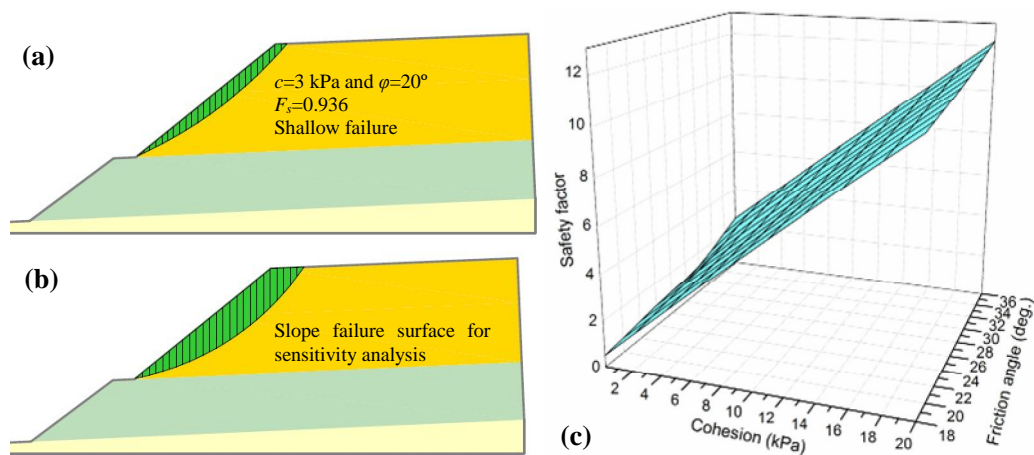


Figure 6. Slope stability analysis results of the experimental unconsolidated slope

The stability of the unconsolidated soil slope is affected by three main factors: a decrease in the shear strength of the unconsolidated soil, an increase of static pore water pressure in the slope and dynamic water pressure generated by interstitial flow. Here, we apply the limit equilibrium method to analyze the stability of the unconsolidated slope with different shear strength parameters (Figure 6). As shown in Figure 6(a), a shallow failure will occur when the shear strength parameters are very low. Sensitivity study for the impact of the shear strength parameters on the safety factor of the slope is conducted based on a certain sliding face (Figure 6(b)). As shown in Figure 6(c), the safety factor decreases with a decrease in the cohesion and friction angle of the unconsolidated soil, which is a linear relationship.

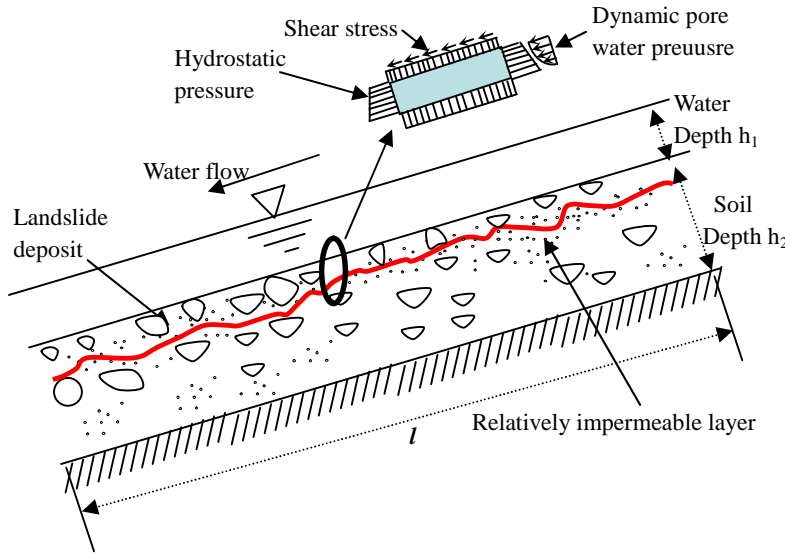
As shown in Figure 6(a) and 6(c), the safety factor of the unconsolidated slope is larger than 1.0 with small soil strength. Comparing with failure phenomenon in experiments, it indicates that the decreasing in shear strength of the unconsolidated soil due to interstitial flow is the essential factor on the failure of the slope; the triggering factor is the hydrodynamic effect by overland flow.

Therefore, widely graded loose soil inducing shallow failure is a process involving the interaction of itself and external conditions. Especially in high mountain areas such as Western China and Italy, thin water flow on the slope surface cannot be overlooked. The slope stability is also analyzed with hydraulic parameters such as peak discharge, flow velocity and depth and coupling with the self-weight. Though Berti (2005) introduced experimental evidence and a numerical model for predicting debris flow initiation through hydraulic calculations, his model still required an empirical formula and is difficult to apply in other areas.

3.2. Model assumption and construction

In order to simplify this problem, we here consider the soil which is in a critical state in 1D failure model. As shown in Figure 7, three simplification assumptions are introduced: (1) the surface water flow is parallel to the

202 slope surface, and the failure face is also parallel; (2) the superficial soil of the unconsolidated soil is in the
 203 saturated stage; and (3) underground water is omitted here. The first assumption is applied in the model to
 204 reduce the complexity of this problem. Through the field investigation (Tang et al., 2012; Zhou et al., 2013) and
 205 laboratory experiments above, we find that the soil is almost completely saturated when shallow failures are
 206 occurring. For the third simplification assumption, it is known that the failure of unconsolidated soil is always in
 207 the valley, which indicates that the main factor is not the increase in the underground water level; thus, the
 208 underground water can be omitted here.



209
 210 **Figure 7.** Simplified assumptions for the stress distribution of unconsolidated soil under hydrodynamic
 211 conditions

212 Detailed force analysis is shown in Figure 7, by assuming that there is an unconsolidated soil failure with a
 213 slope failure depth of a , a surface water flow depth h , a pore water pressure u_w on the failure surface (details are
 214 in section 4.3), a slope angle θ , a cohesion c , a frictional angle φ with saturated soil, dynamic pore water
 215 pressure p_d and water unit weight r_w , and the soil surface friction provided by the surface flow f (details are as
 216 follows), using the **Fredlund** soil strength theory (Fredlund and Rahardio, 1993) and the principle effective
 217 stress, the soil resisting stress at a depth of a can be expressed as follows:

$$218 \quad \tau_f = c + (\sigma - u_w) \tan \varphi, \text{ and } \sigma = (r_{sat} a + r_w h) \cos \theta, \quad u_w = r_w (a + h) \quad (1)$$

219 Combining the above, we can then obtain the resist stress of the unconsolidated soil,

$$220 \quad \tau_f = c + [(r_{sat} a + r_w h) \cos \theta - u_w] \tan \varphi \quad (2)$$

221 and the shear stress can be computed as follows:

$$222 \quad \tau = (r_{sat} a + r_w h) \sin \theta \quad (3)$$

223 Considering the effect of surface water flow, if the shear stress is less than the resist stress of the
224 unconsolidated soil, the slope is stable:

$$225 \quad \tau + f + p_d \leq \tau_f \quad (4)$$

226 If the shear stress is greater than the resisting stress at a depth of $a > 0$, a failure of the unconsolidated slope
227 will occur.

228 (1) Superficial shear stress f

229 Since the 1970s, many scholars have done a lot of research on the overland flow resistance with indoor or
230 outdoor rainfall and erosion tests, by means of different concepts and expressions such as the **Darcy-Weisbach**,
231 **Chezy** and **Manning** friction factor. Due to the complexity of this problem, the Darcy-Weisbach friction factor
232 is mainly used in their models because of its concise form and wide application, suitable for laminar flow and
233 turbulent flow.

234 At present, it is widely accepted that the overland flow resistance in different surfaces can be divided into four
235 sources, namely the grain resistance f_g , form resistance f_f , wave resistance f_w and rainfall resistance f_r . Grain
236 resistance is the resistance formed by soil particles and micro aggregate. The form resistance f_f contains the
237 dissipation of energy by microtopography, vegetation, gravel and so on. Wave resistance f_w forms by vast scale
238 surface deformation. And rainfall resistance is generated by the raindrop.

239 However, these resistances are difficult to measure and quantify in experiments. And the factors may have an
240 interaction effect. So, to simplify, the **Darcy-Weisbach** friction factor λ is chosen to indicate the overflow
241 resistance.

242 According to hydraulics theory, the shear force F that is generated by the surface flow on the slope surface
243 can be calculated as follows:

$$244 \quad f = \lambda \rho v^2 / 8 \quad (5)$$

245 where ρ is the density of water; l is the slope length; λ is the friction loss factor of the hydraulically open channel,
246 and when the thin water flow is laminar flow ($Re < 2000$, Re is Reynolds number), $\lambda = 64/Re$; when it is turbulent
247 flow ($Re > 2000$), $\lambda = 1/[2.1g(3.7R/\Delta)^2]$ (**Nikuradse** empirical formula). $R = A/\chi$ is the hydraulic radius of the
248 cross-section; and Δ is the roughness (slope surface sand diameter), which is usually close to 30-60 mm in a
249 pebble river bed.

250 (2) Dynamic pore water pressure p_d

251 Water pressure in the soil is generally divided into hydrostatic and dynamic pressure. Owing to the dynamic

252 pore water pressure always generated by soil contraction or seepage, the superficial widely graded soil doesn't
 253 have this effect at saturated state with fine particle lost. However, the Reynolds stress from turbulent mixing in
 254 pore water which can be regarded as dynamic water pressure should not be ignored, although it has a small
 255 value (The detailed description is shown in Figure 7). Hotta, et al (2011) constructed a theory formula about
 256 Reynolds stress in debris flow. But in soil, this stress has few literatures to analyze. So we proposed an empirical
 257 formula to forecast this stress. The formula is as follows:

$$258 \quad p_d = A\rho v^2 \quad (6)$$

259 Where p_d is the average Reynolds stress on the cross section of shallow failure layer, kPa; A is empirical
 260 constant, called dynamic pore water pressure coefficient. Generally for the pure water, it is 0.5; ρ is the pore
 261 fluid density, kg/m³; v is pore fluid velocity, m/s. Here, the Reynolds stress is in fact the impact stress by pore
 262 fluid.

263 (3) Sliding face depth a

264 The following simplified form of two-phase flow equations will be used (Cheng et al, 2001; Lu and Cui,
 265 2010a, b). These equations are based on the assumption that the flow is one dimensional and the wall friction
 266 and inertia effect may be neglected. Only the simplest form of interaction between sand grains and water,
 267 namely Darcy's law, is taken into consideration.

$$268 \quad \varepsilon(x, t) = \varepsilon_0(x, 0) + \frac{\lambda}{Tu^* \varepsilon_0(x, 0)} \int_0^t U(\tau) d\tau + O(\lambda^2) \quad (7)$$

269 Where $\varepsilon(x, t)$ stand for the porosity at the depth of x and time of t ; $\varepsilon_0(x, 0)$ is the initial porosity for soil material;
 270 $U(t)$ (unit is cubic meter every second-m³/s) is total flow charge at unit cross-sectional area; t (unit is second) is
 271 the time; L (unit is meter-m) is the soil thickness; λ is a small parameter, employed to obtain an asymptotic
 272 solution; T and u^* are empirical constants.

273 Generally, when we apply this formula, the third term on its left is neglected for simplification. Here, with
 274 fine particle migration and accumulation in some place of slope, the porosity there would be sharply reduced.
 275 Then, we solve the 1D model and get that position x as the blockage place which leads to forming water perched
 276 table and slide face in the end.

277 3.3. Sensitivity analysis of the parameters

278 The physical model above shows that the slope stability condition (safety factor) is related to the grains'
 279 physical characteristics, the slope, surface water flow velocity, surface water flow depth, water flow unit weight,
 280 etc. For a specific type of soil, its physical characteristics are determinate. Therefore, for a physical model, it is

281 important to find out which are the most sensitive factors for slope failure. Here, we assume that the fluid has a
 282 laminar flow, and the safety factor is shown as follows:

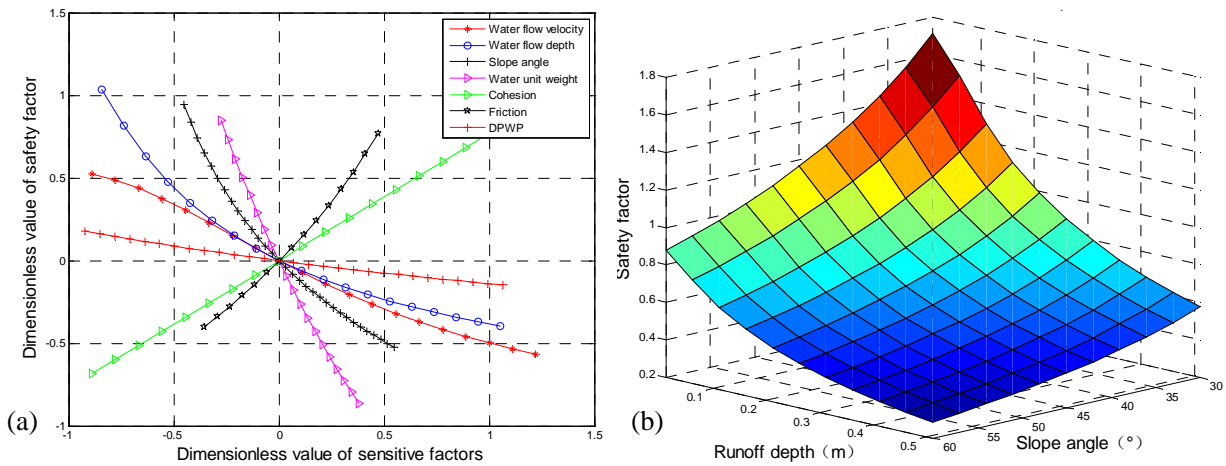
$$283 \quad F_s = \frac{c + (r_{sat} - r_w)a \cos \theta \tan \varphi}{(r_{sat}a + r_w h) \sin \theta + \lambda \rho v^2 / 8 + \Delta \rho v^2 a} \quad (8)$$

284 The values of the model variables that are used for sensitivity analysis are shown in Table 3.

285 **Table 3.** Model variables for sensitivity analysis

| Model variables | Minimum value | Maximum value | Symbol | Unit |
|---------------------------------------|----------------------|--------------------|-----------|-------------------|
| Surface water flow velocity | 0 | 10 | v | m/s |
| Surface water flow depth | 0.01 | 0.4 | h | m |
| Slope angle | 20 | 60 | θ | $^\circ$ |
| Water unit weight | 10^4 | 2×10^4 | r_w | N/m ³ |
| Cohesion | 0 | 2.5 | c | kPa |
| Viscosity | 8.0×10^{-6} | 1×10^{-3} | ν | m ² /s |
| Angle of internal friction | 20 | 50 | φ | $^\circ$ |
| Dynamic pore water pressure parameter | 0 | 3 | A | - |

286
 287 Considering the safety factor F_s to be a function of the sensitive factors, we can use the usual form $S_i = \Delta F_s / \Delta x_i$
 288 to conduct sensitivity analysis (Δ represents a tiny variable; F_{si} , x_i respectively represent the i th safety factor and
 289 a sensitive factor influencing the F_s . To compare all of the factors, which have different units, the common
 290 method is to normalize S_i to $I_i = \frac{\Delta F_s / F_{si}}{\Delta x_i / x_i}$. A high absolute value of I_i stands for the high sensitivity of the i th
 291 factor. Through the relationships between $\Delta F_s / F_{si}$ and $\Delta x_i / x_i$ (Figure 8), we can find how the model parameter
 292 affects the initiation of the debris flow.



293
 294 **Figure 8.** The relationship between model I variables and safety factor: (a) Sensitivity analysis results of the
 295 model variables; and DPWP stands for ‘dynamic pore water pressure’; (b) the relationship between safety factor

296 and surface water flow depth and slope angle.

297 As shown in Figure 8(a), we can obtain that the sensitivity, from high to low, is as follows: water unit weight,
298 slope angle, flow depth, angle of internal friction, cohesion, flow velocity. The cohesion and internal friction
299 angle, which have negative correlation with the slope stability, make a certain contribution and cannot be
300 ignored. Besides the slope angle, which is well known for its important effect, the following flow depth and
301 velocity indicate that the thin water flow that can produce the shear stress should also not be omitted in the
302 model, especially as, when superficial water flow runs down the slope, it can carry fine particles away with
303 cohesion decreasing and pore water density increasing, and leading to slope instability in the end.

304 The sensitivity analysis of variables in this model can be used to guide its application and choose suitable
305 variable. For example, superficial water flow velocity is sensitive for safety factor which is always neglected
306 due to its small value. Moreover, this model is derived from soil mechanics and experimental results and is
307 suitable for widely graded and unconsolidated slope under rainfall or thin water flow condition.

308 4. Simulation of laboratory testing

309 According to the artificial rainfall test for the unconsolidated slopes, the presented model is verified by
310 laboratory. And the values of the model parameters are shown in Table 4.

311 Due to the subsurface flow velocity difficult to measure, shallow with thin water flow condition is used
312 here to verify this model. Firstly, we assume the soil porosity is distributing in following form.

$$313 \quad \varepsilon_0(x,0) = a - b \sin\left(\frac{cx - dL}{L}\right)\pi \quad (9)$$

314 where a , b , c and d are empirical constants.

315 With equation (7) and the boundary condition (9), we can get the porosity distribution at $t=1200s$ in Figure 9.
316 Along the soil depth, soil porosity changes circularly from low to high. As we know, shallow failure is all
317 occurring in the shallow layer. So the low porosity 0.1 in depth 0.05 cm below is regard as the position of
318 sliding.

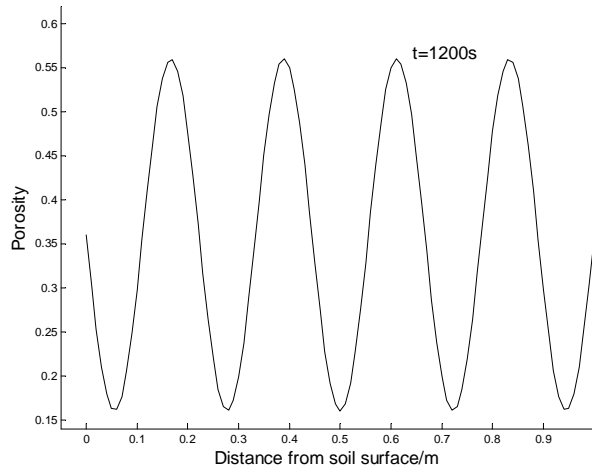
319 Moreover, under rainfall and thin water flow conditions, top layer soil is regarded in a saturated state. And
320 these phenomena are also observed in the tests shown in Figure 4 and Cui et al 2014). However, considering the
321 superficial water flow effect, which leads to the soil coarsening, the cohesion c in thin water flow condition is
322 taken as zero, comparing with the rainfall condition $c=22.3kPa$. The actual variables are shown in Table 4.
323 Through the formula (8), the safety factors under no-runoff and runoff conditions are respectively 32.51

324 (no-runoff, $c=22.3\text{kPa}$, $h=0\text{ m}$, other parameters are the same as Table 3) and 0.19 ($c=0\text{ kPa}$, with runoff,
 325 detailed parameters are shown in Table 4). Thus, the results show that the slope is stable except small scale
 326 shallow failure under the no-runoff condition and fails with the runoff condition, which is consistent with the
 327 experiment results and indicates the rationality of this hydrodynamic model.

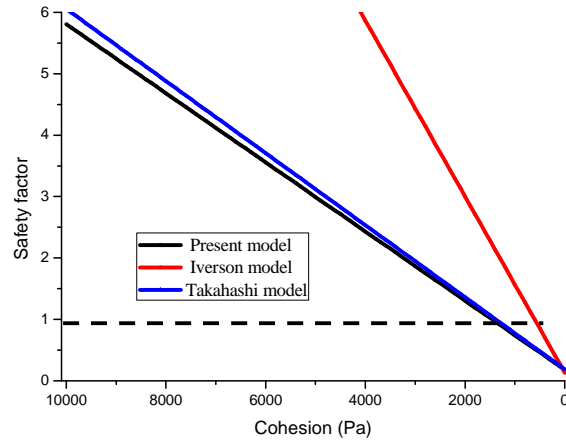
328 **Table 4.** Model variables that are used to simulate laboratory testing

| Variable Name | Unit | Value (Rainfall condition) | Value (Thin water flow condition) |
|---|------|----------------------------|-----------------------------------|
| Soil unit weight r_{sat} | N/m | 2.10×10^4 | 2.10×10^4 |
| Water unit weight r_w | N/m | 1.00×10^4 | 1.00×10^4 |
| Slope angle θ | ° | 42 | 42 |
| Cohesion c | kPa | 0 | 22.3 |
| Angle of internal friction φ | ° | 32.3 | 32.3 |
| Water flow depth h | m | 0 | 0.05 |
| Water flow velocity v | m/s | 0 | 1.70 |
| Channel width w | m | 0.40 | 0.40 |
| Dynamic pore water pressure coefficient A | - | 0 | 0.5 |

329
 330 To be sure, with the runoff condition, the fluid is regarded as laminar flow ($Re \approx 1214$). And generally, soil
 331 internal friction is less influenced by water content. So the soil parameter with no-runoff is the same as the
 332 runoff condition except for the cohesion.



333
 334 **Figure 9.** Porosity distribution in 1D model ($T=1.0$, $u^*=0.04$; $a=0.36$; $b=0.2$; $c=1.0$; $d=0.0$; $L=1$)



335

336 **Figure 10.** Safety factor under different cohesion with other condition unchanged

337 With sliding depth and other model conditions unchanged, the relationships between safety factors with
 338 cohesion are constructed by Takahashi model (Takahashi, 2007), Iverson model (Iverson, 1997) and model in
 339 this paper. From Figure 10, we can get that there are some differences among three models. Specially, Iverson
 340 model which is only considering the underground water not the superficial water has the maximum gap with our
 341 model. Though Takahashi model has little gap but it omits the dynamic pore water pressure and can't compute
 342 the sliding face depth. And not only the shear force and dynamic pore water pressure by thin water flow, but also
 343 its sand-carrying effect is considered in the hydrodynamic model, which shows a conservative and safe method
 344 for slope safety analysis.

345 Despite the cohesion of coarse soil is though as zero with three models applying, it is in fact not zero when
 346 the slope fails. So the varied cohesion of coarse soil in practice is should be considered in the future.

347 5. Conclusion and discussion

348 5.1. Conclusion

349 To study the shallow failure mechanism, experiments designed considering the rainfall and thin water flow,
 350 the important role of the hydrodynamic effect has been identified and clearly understood. On one hand, overland
 351 flow increases the unit weight of water flow, which will increase the shear effect to the slope; on the other hand,
 352 interstitial flow carries away the fine particles which lead to the soil coarsening and soil strength decreasing.
 353 Meanwhile, fine particle would migrate, depose at some position of soil pore network and form relatively
 354 impermeable layer which can be regard as sliding face for shallow failure. However, coupling effects above are
 355 sudden, invisible therefore always omitted in practice. Moreover, a theoretical model for shallow failure
 356 considering the hydrodynamic effect is proposed and verified by test data. Especially, the simulation results

357 show that this model is much more appropriate for unconsolidated soil failure analysis by considering the
358 hydrodynamic condition and more handy due to the simplification on other soil properties.

359 *5.2. Discussion*

360 **Shallow failure is a common disaster which could transform into debris flow on slope. Although water flow is**
361 **considered as the key to trigger debris flow in a channel or gully, hydrodynamic effects by thin water flow on**
362 **slope surface** which add the shear force along the slope and lead to soil strength decreasing due to fine particles
363 migrating and forming locally impermeable layer, have not been well known in the current literature (Iverson et
364 al., 2010, 2011; Huang et al., 2009, 2010; Lade, 2010). The surface runoff cause soil failure in this way is
365 usually regarded as an erosion effect. In practice, this process (soil failure, from sliding to flowing) is sudden
366 and relatively complex in nature (Malet, 2005). Moreover, unconsolidated soil with a loose structure is prone to
367 be dispersed by water flow and this effect is commonly mistaken as erosion or entrainment. So the findings in
368 this paper will provide a new angle on the debris flow initiation and unconsolidated soil failure.

369 Based on hydraulic theory, an unconsolidated soil failure model has been established which incorporates the
370 hydrodynamics shear stress and pore water pressure. This model has improved on a setback in the hydraulic and
371 soil mechanics coupling model (Takahashi, 2007; Iverson, 1997), which omits the dynamic pore water pressure
372 and the computation of sliding face.

373 In addition, in the typical slope analysis, the sliding face can always be determined by geological analysis
374 such as the soft layer or stability computation. However, the sliding face is random and shallowly existed in the
375 widely graded loose soil. In this study, the sliding face is assumed to be a plane locating at shallow depth
376 through porosity analysis. In the future, the sliding face shall be defined using a precise numerical model rather
377 than estimation. Moreover, though our study on the shallow failure which have considered the hydrodynamic
378 effects can provide a physical basis for understanding the triggering threshold, it must be admitted that the
379 unconsolidated soil failure is rather complex and the simplification and assumption made in our model should
380 be explored in our future study along the way.

381 **Acknowledgments**

382 We gratefully acknowledge the support of the Key Deployment Project of the Chinese Academy of Sciences
383 (KZZD-EW-05-01), the National Natural Science Foundation of China (41102194, 41030742), the Science
384 Foundation for Excellent Youth Scholars of Sichuan University (2013SCU04A07) and the China Postdoctoral

385 Science Foundation Funded Project (2012T50785).

386 **References**

387 Bagnold, R. A.: Experiments on a gravity-free dispersion of large solid spheres in a Newtonian fluid under shear.
388 Proceedings of the Royal Society of London. Series A. Mathematical and Physical Sciences, 225(1160),
389 49-63, 1954.

390 Berti, M., Simoni, A.: Experimental evidences and numerical modelling of debris flow initiated by channel
391 runoff, *Landslides*, 2, 171-182, 2005.

392 Bryan, R. B.: Soil erodibility and processes of water erosion on hillslope, *Geomorphology*, 32(3), 385-415,
393 2000.

394 Chen, X. Q., Cui, P., Feng, Z. L., Chen, J. and Li, Y.: Artificial rainfall experimental study on landslide
395 translation to debris flow, *Yanshilixue Yu Gongcheng Xuebao/Chinese Journal of Rock Mechanics and*
396 *Engineering*, 25(1), 106-116. 2006.

397 Cheng, C. M., Qingming, T. and Fujiao, P.: On the mechanism of the formation of horizontal cracks in a vertical
398 column of saturated sand. *Acta Mechanica Sinica*, 17(1), 1-9, 2001.

399 Cui, P.: Study on condition and mechanisms of debris flow initiation by means of experiment, *Chinese Science*
400 *Bulletin*, 37, 759-763, 1992.

401 Cui, P., Guo, C. X., Zhou, J. W., Hao, M. H. and Xu, F. G.: The mechanisms behind shallow failures in slopes
402 comprised of landslide deposits, *Engineering Geology*, doi: <http://dx.doi.org/10.1016/j.enggeo.2014.04.009>,
403 2014.

404 Fredlund, D. G. and Rahardjo, H. (Eds.): *Soil mechanics for unsaturated soils*, John Wiley & Sons, USA, 1993.

405 Gabet, E. J, and Mudd, S. M.: The mobilization of debris flows from shallow landslides, *Geomorphology*, 74,
406 207-218, 2006.

407 Gregoretti, C. and Fontana, G. D.: The triggering of debris flow due to channel-bed failure in some alpine
408 headwater basins of the Dolomites: Analyses of critical runoff, *Hydrological Processes*, 22, 2248-2263, 2008.

409 Hotta, N.: I Pore water pressure distributions of granular mixture flow in a rotating mill. *Debris-Flow Hazards*
410 *Mitigation: Mechanics, Prediction and Assessment*, edited by: Genevois, R., Hamilton, DL, and Prestininzi,
411 A., Casa Editrice Universita La Sapienza, Roma, 319-330, 2011.

412 Huang, C. C., Lo, C. L., Jang, J. S. and Hwu, L. K.: Internal soil moisture response to rainfall-induced slope
413 failures and debris discharge, *Engineering Geology*, 101, 134-145, 2008.

414 Huang, C. C., Ju, Y. J., Hwu, L. K. and Lee, J. L.: Internal soil moisture and piezometric responses to

415 rainfall-induced shallow slope failures, *Journal of Hydrology*, 370, 39-51, 2009.

416 Iverson, R. M., Reid, M. E. and LaHusen, R. G.: Debris-flow mobilization from landslides 1, *Annual Review of*
417 *Earth and Planetary Sciences*, 25, 85-138, 1997.

418 Iverson, R. M., Reid, M. E., Iverson, N. R., LaHusen, R. G., Logan, M., Mann, J. E. and Brien, D. L.: Acute
419 sensitivity of landslide rates to initial soil porosity, *Science*, 290(5491), 513-516, 2000.

420 Iverson, R. M., Reid, M. E., Logan, M., LaHusen, R. G., Godt, J. W. and Griswold, J. P.: Positive feedback and
421 momentum growth during debris-flow entrainment of wet bed sediment, *Nature Geoscience*, 4(2), 116-121,
422 2011.

423 Lade, P. V.: The mechanics of surficial failure in soil slopes, *Engineering Geology*, 114, 57-64, 2010.

424 Lu, X. B. and Cui P.: A study on water film in saturated sand, *International Journal of Sediment Research*, 25(3),
425 221-232, 2010a.

426 Lu, X. B., Cui, P., Hu, K. H. and Zhang, X. H.: Initiation and development of water film by seepage, *Journal of*
427 *Mountain Science*, 7(4), 361-366, 2010b.

428 Malet, J. P., Laigle, D., Remaître, A. and Maquaire, O.: Triggering conditions and mobility of debris flows
429 associated to complex earthflows, *Geomorphology*, 66(1), 215-235, 2005.

430 Takahashi, T.: *Debris Flow: Mechanics, Prediction and Countermeasures*. Taylor & Francis, 2007.

431 Tang, C., Van Asch, T. W. J., Chang, M, Chen, G. Q., Zhao, X. H. and Huang, X. C.: Catastrophic debris flows
432 on 13 August 2010 in the Qingping area, southwestern China: The combined effects of a strong earthquake
433 and subsequent rainstorms, *Geomorphology*, 139, 559-576, 2012.

434 Tognacca, C., Bezzola, G. R. and Minor, H. E.: Threshold criterion for debris-flow initiation due to channel bed
435 failure, In: *Proceedings of the 2nd international conference on debris flow hazards mitigation*, Taipei, Taiwan,
436 16-18 August 2000, 89-97, 2000.

437 Wang, Z. Y. and Zhang X. Y.: Initiation and Laws of Motion of Debris Flow, In: *Proceedings of the*
438 *International Symposium on the Hydraulics and Hydrology of Arid Lands in conjunction with the 1990*
439 *National Conference on Hydraulic Engineering*, San Diego, California, July 30-August 3, 1990.

440 Zhou, J. W., Cui, P., Yang, X. G., Su, Z. M. and Guo, X. J.: Debris flows introduced in landslide deposits under
441 rainfall conditions: the case of Wenjiagou gully, *Journal of Mountain Science*, 10, 249-260, 2013.